



Isotopic characterization of lifetime movement by two demersal fishes from the northeastern Gulf of Mexico

Julie L. Vecchio^{1,2,*}, Jenny L. Ostroff^{1,3}, Ernst B. Peebles¹

¹College of Marine Science, University of South Florida, 830 1st St South, St. Petersburg, FL 33701, USA

²Present address: Florida Fish and Wildlife Research Institute, 100 8th Avenue SE, St. Petersburg, FL 33701, USA

³Present address: NOAA Fisheries, 263 13th Ave S, St. Petersburg, FL 33701, USA

ABSTRACT: An understanding of lifetime trophic changes and ontogenetic habitat shifts is essential to the preservation of marine fish species. We used carbon and nitrogen stable isotope values ($\delta^{13}\text{C}$ and $\delta^{15}\text{N}$) recorded within the laminar structure of fish eye lenses, reflecting both diet and location over time, to compare the lifetime trends of 2 demersal mesopredators. Tilefish *Lopholatilus chamaeleonticeps* inhabit burrows on the outer continental shelf, which results in exceptional site fidelity. Red grouper *Epinephelus morio* are spawned on the middle to outer continental shelf, move to the inner shelf for the juvenile period, and return offshore upon sexual maturity. Both species inhabit the eastern Gulf of Mexico, a region with a distinctive offshore–inshore gradient in background $\delta^{13}\text{C}$ values. Within individual tilefish ($n = 36$), sequences of $\delta^{13}\text{C}$ values and $\delta^{15}\text{N}$ values had strong, positive correlations with eye-lens diameter, and strong correlations between the 2 isotopes (mean Spearman $r = 0.86$), reflecting an increase in trophic position with growth and little lifetime movement. In red grouper ($n = 30$), $\delta^{15}\text{N}$ values positively correlated with eye-lens diameter, but correlations between $\delta^{15}\text{N}$ and $\delta^{13}\text{C}$ were weak (mean Spearman $r = 0.29$), suggesting cross-shelf ontogenetic movements. Linear mixed model results indicated strong relationships between $\delta^{15}\text{N}$ and $\delta^{13}\text{C}$ values in tilefish eye lenses but no convergence in the red grouper model. Collectively, these results are consistent with previously established differences in the life histories of the 2 species, demonstrating the potential utility of eye-lens isotope records, particularly for investigating the life histories of lesser-known species.

KEY WORDS: Stable isotopes · Fish eye lenses · Fish movement · $\delta^{13}\text{C}$ · $\delta^{15}\text{N}$ · Trophic growth

Resale or republication not permitted without written consent of the publisher

1. INTRODUCTION

Many marine fish species undergo ontogenetic shifts in both location and diet, using different habitats and food resources during juvenile and adult life stages (e.g. Dahlgren & Eggleston 2001, Saul et al. 2012, Kurth et al. 2019). While an understanding of the habitat needs for each life stage is important, the extent of movement may be difficult to assess in many species. Stable isotope data can be used to interpret both species movements and trophic position (Ainsworth et al. 2015, Grüss et al. 2016). An increase in $\delta^{15}\text{N}$ values with body size is a common

phenomenon among marine predators, and has been termed ‘trophic growth’ (Wallace et al. 2014, Curtis et al. 2020, Liu et al. 2020). Within a single species, individuals often feed at higher trophic positions as they grow, resulting in trophic growth (e.g. summer flounder *Paralichthys dentatus*, Buchheister & Latour 2011; boreo-Atlantic armhook squid *Gonatus fabricii*, Golikov et al. 2018; yellowfin tuna *Thunnus albacares*, Graham et al. 2007). Although trophic fractionation can be variable, $\delta^{15}\text{N}$ values in marine mesopredator tissues increase by approximately 2.3–3.4‰ and $\delta^{13}\text{C}$ values increase by 1.9–2.3‰ with each trophic step (Post 2002, McCutchan et al. 2003, Mo-

*Corresponding author: jlvsses@gmail.com

han et al. 2016, Eddy 2019). Tissue $\delta^{13}\text{C}$ values can be useful for indicating basal-resource dependence (Fry & Wainright 1991, Dance et al. 2018). The $\delta^{13}\text{C}$ values of subtropical marine phytoplankton have been found to be between 3.7 and 6‰ more negative than those of benthic primary producers (Moncreiff & Sullivan 2001, Grippo et al. 2011, Dance et al. 2018).

One factor that complicates the interpretation of individual isotopic composition bulk tissues for trophic position and basal-resource dependence in marine consumers is geographic variation in isotopic baselines. Spatial variations in stable isotope compositions (isoscaples) have been established for a number of marine regions, and these trends are reflected in the tissues of predators moving through these areas (MacKenzie et al. 2011, Simpson et al. 2019, Trueman et al. 2019). Whereas changes in trophic position will result in changes to isotope values over time, baseline isotope values can have a similar effect on the isotopic composition of tissues assimilated during movement. For example, if a fish were to remain stationary while increasing trophic position during life, then both $\delta^{15}\text{N}$ values and $\delta^{13}\text{C}$ values would be expected to increase concomitantly as a function of positive trophic fractionation. Based on trophic discrimination factors for each isotope, the average slope of this relationship would be expected to range from 1.0 to 1.7 in marine mesopredators (Post 2002, McCutchan et al. 2003, McMahan et al. 2010). In contrast, if the baseline values of the isotopes of interest ($\delta^{15}\text{N}$ and $\delta^{13}\text{C}$, in this case) trend in different geographic directions and the fish has moved across these opposing trends, then the consistent linear relationship between the isotope values would be degraded or lost.

During organismal growth and cell maintenance, new isotopic information is continuously incorporated into various tissue types, often at distinct rates (Sweeting et al. 2005, Buchheister & Latour 2010, Heady & Moore 2013). Internal eye-lens layers (laminae) experience little or no turnover and function as a conservative record of the isotopic histories within each individual (Wallace et al. 2014, Nielsen et al. 2016, Simpson et al. 2019, Curtis et al. 2020). Peebles & Hollander (2020) reviewed fish eye-lens physiology as it relates to stable isotopes. In short, the record-keeping behavior of eye lenses arises from lifetime conservation of optical proteins called crystallins. New protein synthesis within individual cells is not possible after cell formation and the subsequent apoptosis (removal) of cellular organelles, which improves the optical properties of the cells (Lynnerup et al. 2008, Rinyu et al. 2020). This selec-

tive apoptosis results in preservation of the original organic material within successively created laminae (Nicol 1989, Lynnerup et al. 2008, Stewart et al. 2013, Nielsen et al. 2016). A captive diet-switch study (Granneman 2018) documented isotopic shifts within fish eye lenses that mirrored an isotopic shift in the feed, confirming that a change in diet is reflected in the fish eye-lens record.

The continental shelf offshore Florida's Gulf of Mexico coast (West Florida Shelf) consists of gradually sloping soft sediment interspersed with limestone reefs and outcroppings (Locker et al. 2010, Hine & Locker 2011). Tilefish *Lopholatilus chamaeleonticeps* and red grouper *Epinephelus morio* are both large, demersal predators common in the northeastern Gulf of Mexico. Both species excavate soft sediments (Scanlon et al. 2005, Ellis et al. 2017) and associate closely with the burrows or depressions that they create (Able et al. 1982, Coleman et al. 2011, Ellis 2019, Grasty et al. 2019). Juveniles of both species consume benthic invertebrates (Brule & Canche 1993, Steimle et al. 1999) and the proportion of fish in the diet increases as individuals grow (Grimes et al. 1986, Weaver 1996). However, there are notable distinctions between the life histories of the 2 species in the northeastern Gulf of Mexico.

Individual tilefish create and maintain vertical burrows in clay sediments (Grossman et al. 1985, Grimes et al. 1986, Able et al. 1987) near the edge of the continental shelf. Smaller individuals are observed near smaller burrows, suggesting that they remain near the same burrow over many years (Able et al. 1982, Grimes 1983, Grimes et al. 1986, Fisher et al. 2014). Captive-reared tilefish have been observed settling to the bottom and beginning to dig by 1.5 cm standard length (Fahay 1983). Because this species rarely consumes migratory prey (Steimle et al. 1999), $\delta^{13}\text{C}$ values and $\delta^{15}\text{N}$ values of lens protein should reflect local conditions at a single location throughout the lifespan of an individual.

Juvenile red grouper are found on the inner continental shelf (<30 m depth), where they use rocky reef habitats (Bullock & Smith 1991). Adult red grouper maintain depressions in soft sediment veneers overlying limestone outcrops on the middle to outer continental shelf (Coleman et al. 2010, Wall et al. 2011, Grasty et al. 2019). Tagging studies indicate that most adult red grouper move little over a 1–2 yr period (Burns & Froeschke 2012, Farmer & Ault 2014). However, recaptures of individuals that did move were in deeper water than the depth of original tagging (Moe 1969, Burns 2009, Saul et al. 2012). Based on these data and the relationship between size and capture

depth, it is clear that red grouper use different habitats during life (Moe 1969, Johnson & Collins 1994, Grüss et al. 2017). The existence of ontogenetic habitat shifts thus distinguishes red grouper from tilefish.

Baseline trends in fish tissue $\delta^{15}\text{N}$ values and $\delta^{13}\text{C}$ values on the West Florida Shelf are consistent among years, seasons, and species, allowing for the delineation of regional isoscapes (Fig. 1A; Radabaugh et al. 2013, Radabaugh & Peebles 2014, Huelster 2015). Values of $\delta^{15}\text{N}$ are highest in the northwestern extreme and lowest on the southern end of the West Florida Shelf, which is consistent with high rates of riverine input to the north and elemental nitrogen fix-

ation by diazotrophs to the south (McClelland et al. 2003, O'Connor et al. 2016). Trends in $\delta^{13}\text{C}$ values on the West Florida Shelf are orthogonal (rotated 90°) to those of $\delta^{15}\text{N}$ values, with highest values in shallow, clear waters where benthic primary producers are more abundant (Radabaugh et al. 2013). Because of this orthogonal relationship, movement across these 2 isoscapes ($\delta^{15}\text{N}$ and $\delta^{13}\text{C}$) decouples temporal trends in $\delta^{13}\text{C}$ values and $\delta^{15}\text{N}$ values within the eye lenses of an individual fish.

Stable isotope values have been used in a variety of settings with a single species or a small group of species as models for life history and autecology (Tallamy & Pesek 1996, Holtum & Winter 2014, Ogston et al. 2016). We used profiles of eye-lens $\delta^{13}\text{C}$ values and $\delta^{15}\text{N}$ values from tilefish and red grouper as models of distinct demersal mesopredator life histories within a similar geographic region. We compared the isotopic histories of burrow-inhabiting tilefish, which have lifelong site fidelity, to those of red grouper, which move long distances as they grow and mature. By using these 2 species as contrasts between a lifetime at a single location and a lifetime of ontogenetic movement, we can use lifetime isotopic patterns to interpret movement of other species living in regions with similar isotopic contrasts, including species for which gaps exist in our understanding of their life history.

2. MATERIALS AND METHODS

2.1. Sample collection and preparation

We obtained 36 adult tilefish from the University of South Florida's benthic longline surveys (Murawski et al. 2018) and 30 red grouper from the Southeast Area Monitoring and Assessment Program (SEAMAP) groundfish trawl surveys (Eldridge 1988). Tilefish were collected from the northern West Florida Shelf and adjacent areas to the west (Fig. 1B) in water depths of 178–375 m. Red grouper were collected from the northern and central West Florida Shelf (Fig. 1B) in water depths of 10–40 m. Tilefish were measured to the nearest cm fork length (FL), dissected, and sexed macroscopically at sea. Red grouper were measured to the nearest mm FL and dissected at sea but were not sexed due to the difficulty of macroscopic sex designation in this species (Lowerre-Barbieri et al. 2014). All specimens were beyond the length at 50% maturity (SEDAR 2011, Lombardi-Carlson 2014). Red grouper are protogynous, with 50% transition to male at 743 mm

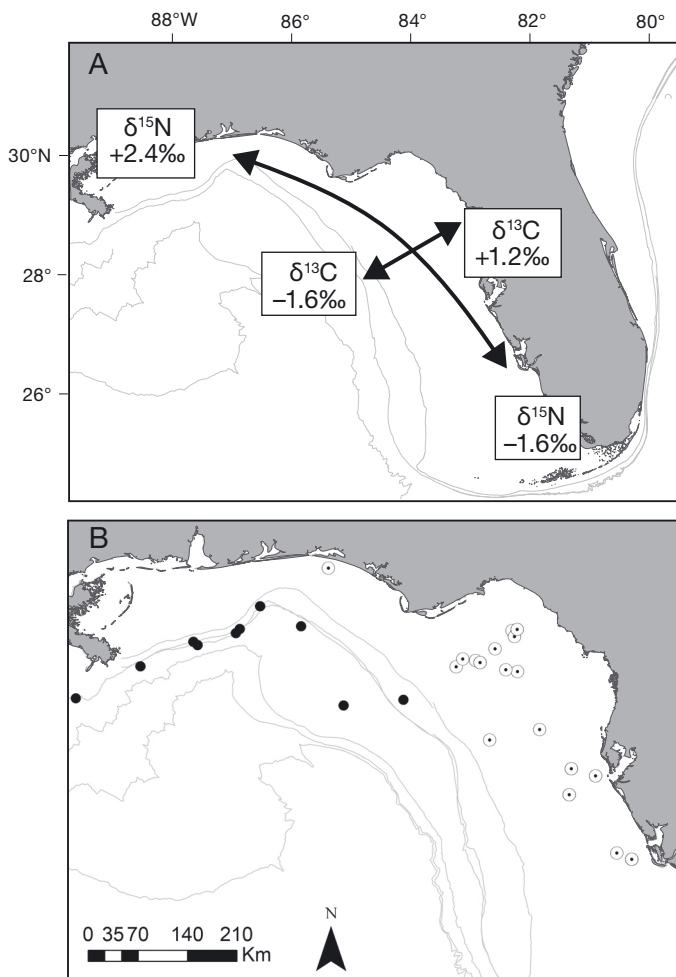


Fig. 1. Region of interest, northeastern Gulf of Mexico. (A) Generalized background isotope (isocape) trends (based on Radabaugh & Peebles 2014 and Peebles & Hollander 2020). Values in this context represent deviation from mean values; they do not represent organismal tissue values of $\delta^{13}\text{C}$ or $\delta^{15}\text{N}$. Arrows cross approximately at mean values in both isotopes. (B) Collection locations for all fish in the study (white symbols: red grouper; black symbols: tilefish). More than 1 fish was collected at several of the mapped locations. Bathymetry markings are 100, 200, 1000, 2000, and 3000 m

FL and 11.5 yr (Lowerre-Barbieri et al. 2014). Otoliths were cleaned of tissue before storing dry at room temperature, and whole eyes were frozen at -20°C until analysis.

Sagittal otoliths were aged by counting annuli under transmitted light microscopy using an Olympus SZX12 zoom stereomicroscope. Each species was aged according to the method employed by the Florida Fish and Wildlife Conservation Commission Age and Growth Lab, which assisted on this project. Tilefish otoliths were thin-sectioned and attached to a microscope slide, and annuli were counted (Lombardi-Carlson & Andrews 2015). Red grouper otoliths were aged whole in a water-filled petri dish (Johnson & Collins 1994). Data on age and length were combined to confirm maturity status (Tables S1 & S2 in the Supplement at www.int-res.com/articles/suppl/m657p161_supp.pdf; SEDAR 2011, Lombardi-Carlson 2014).

We dissected and processed eye lenses according to Wallace et al. (2014) immediately prior to isotope analysis. We thawed whole eyes individually, removed the lens from the lens capsule, placed each lens on a glass petri dish, and measured eye-lens diameter (ELD) to the nearest 0.05 mm using an ocular micrometer in an Olympus SZX12 zoom stereomicroscope at 10 \times magnification. We delaminated each lens using 2 fine-tipped forceps under 10–50 \times magnification and recorded the ELD after removal of each lamina. We identified each lamina based on its diameter midpoint (midpoint between successive ELDs). The lens core (<1 mm diameter) was the final tissue in the analyzed series. De-ionized water was used sparingly for tilefish eye-lens delamination, but red grouper eye lenses were submerged in water for delamination. The 2 methods have been shown to result in comparable isotopic values (Meath et al. 2019). Lamina material became desiccated in <1 h at 25°C .

2.2. Isotope analysis

For isotope analysis, we weighed 200–600 μg of eye-lens material from each lamina to the nearest μg on a Mettler-Toledo precision microbalance. We used a Carlo-Erba NA2500 Series II Elemental Analyzer combustion furnace coupled to a continuous-flow ThermoFinnigan Delta+XL isotope ratio mass spectrometer to measure $^{13}\text{C}/^{12}\text{C}$, $^{15}\text{N}/^{14}\text{N}$, and C:N ratios in duplicate at the University of South Florida College of Marine Science in St. Petersburg, Florida. Calibration standards (mean \pm SD) were NIST 8573 ($-26.39 \pm$

0.09‰ and $-4.52 \pm 0.12\text{‰}$ for $\delta^{13}\text{C}$ and $\delta^{15}\text{N}$ values, respectively) and NIST 8574 L-glutamic acid ($37.63 \pm 0.10\text{‰}$ and $47.57 \pm 0.22\text{‰}$ for $\delta^{13}\text{C}$ and $\delta^{15}\text{N}$ values, respectively) standard reference materials. Results are presented in delta notation (δ , in ‰) relative to international standards Vienna Pee Dee Belemnite for carbon and air for nitrogen:

$$\delta X = \left(\frac{R_{\text{sample}}}{R_{\text{standard}}} - 1 \right) \times 1000 \quad (1)$$

where X is either ^{13}C or ^{15}N and R is the isotopic ratio of interest ($^{13}\text{C}/^{12}\text{C}$ or $^{15}\text{N}/^{14}\text{N}$). Analytical precision, obtained by replicate measurements of NIST 1577b bovine liver, was 0.20‰ for $\delta^{13}\text{C}$ values and $\pm 0.30\text{‰}$ for $\delta^{15}\text{N}$ values (maximum standard deviations of $n = 300$ replicates).

2.2.1. Eye-lens isotope data analysis

All data analyses were conducted in R statistical software version 3.6.1 (R Core Team 2019). Eye-lens isotope profiles represent changes in the eye-lens $\delta^{13}\text{C}$ values and $\delta^{15}\text{N}$ values throughout the lifetime of each fish, with the innermost lamina representing the youngest age (postlarval period) and the outermost lamina representing age at capture. Eye lenses do not contain known age marks. Therefore, we used the best-fit regression to relate ELD to FL for each species. For tilefish, we used the linear regression $\text{FL (cm)} = 6.03 \times \text{ELD (mm)}$ ($F = 1220$, $R^2 = 0.97$, $p < 0.001$; $n = 36$, FL range = 48–99 cm). The regression was constructed using maximum ELD and FL for the individuals used for this study. For red grouper, we used the logarithmic regression $\text{FL (cm)} = e^{(e+0.21 \times \text{ELD})}$ ($F = 510$, $R^2 = 0.84$, $p < 0.01$; $n = 99$, FL range = 4.4–80.5 cm). The regression was constructed using the individuals from the current study as well as 69 juveniles ranging from 4.4 to 30.0 cm FL.

We calculated mean and standard error for the eye-lens $\delta^{13}\text{C}$ values and $\delta^{15}\text{N}$ values of each species. Subsequently, we used the PERMDISPER and PERMANOVA routines in R (package 'vegan,' Oksanen et al. 2019) to compare $\delta^{13}\text{C}$ values to $\delta^{15}\text{N}$ values from the 468 individual tilefish eye-lens laminae with the 406 red grouper eye-lens laminae.

For each species, we measured the fit of a logarithmic curve $\delta X = a + b \times \ln(\text{ELD})$ where a is the parameter controlling the curve location on the y -axis and b is the parameter controlling curve shape. This model was chosen as a version of growth equations commonly used in fish (von Bertalanffy 1938, Ricker 1975). Regression trends can be attributed to

changes in trophic position with somatic growth. Substantial deviation from this curve can be attributed to movement across the background isoscape or change in basal-resource dependence. We used the 'lmer' routine in the 'lme4' package in R (Bates et al. 2015) to construct linear mixed effects models comparing $\delta^{13}\text{C}$ values to $\delta^{15}\text{N}$ values in each species, using individual fish as a random effect. We used the 'permanova.lmer' function in the package 'Predictmeans' (Luo et al. 2020) to compute a permuted p-value for the overall model in each species.

2.2.2. Isotope interpretations: movement vs. trophic position increase for individual fish

We used a series of correlations to distinguish between the influence of changing trophic position and movement within individual eye-lens isotope profiles. We identified all possible isotopic outcomes that would be associated with different combinations of geographic movement (Radabaugh & Peebles 2014) or trophic position increase with growth (Fry 2006, Wallace et al. 2014) at the individual level (Fig. 2). In Fig. 2, gray-shaded cells represent these trends (positive, negative, or neutral), as indicated by significant departures of lifetime regression slopes from zero. The potential geographic and trophic explanations for these trends are presented in unshaded cells. For example, an individual may have a positive lifetime trend (+, shaded gray) in $\delta^{15}\text{N}$ values or $\delta^{13}\text{C}$ values for 3 reasons: (1) it moved

		Geographic movement		
		+	-	0
Trophic position	+	+	+ 0 -	+
	-	+ 0 -	-	-
	0	+	-	0

Fig. 2. Interpretation of lifetime trends (regression slopes, shaded gray) in either $\delta^{13}\text{C}$ or $\delta^{15}\text{N}$ within fish eye lenses, with trophic and geographic interpretations presented in unshaded cells. Lifetime isotopic trends (regression slopes) can be positive, negative, or neutral (+, -, or 0). Mixed inputs can result in variable observations due to differences in relative size of the change in location or trophic position. See Section 2.2.2 for more details

in a positive direction along a baseline isotopic gradient while increasing its trophic position, (2) it increased its trophic position without substantial movement, or (3) it moved in a positive direction along a baseline isotopic gradient without substantially changing its trophic position.

In addition to these lifetime trends, we considered another suite of relationships (via Spearman correlation, r_s) that provided additional information; the conceptual outcomes of these are presented in Table 1 (which is analogous to Fig. 2, but is based on correlation). Specifically,

(1) we correlated $\delta^{15}\text{N}$ values with ELD within individual eye-lens profiles to determine whether trophic growth or movement along the $\delta^{15}\text{N}$ gradient had occurred (Hansson et al. 1997);

(2) we correlated $\delta^{13}\text{C}$ values with ELD within individual eye-lens profiles to determine whether movement along the $\delta^{13}\text{C}$ baseline had occurred or if basal-resource dependence had changed (Fry & Wainright 1991, Radabaugh & Peebles 2014); and

(3) we correlated $\delta^{13}\text{C}$ values with $\delta^{15}\text{N}$ values within individual eye-lens profiles to represent site fidelity, with strong correlations indicating high site fidelity during life (McCutchan et al. 2003, Meath et al. 2019).

Individuals with strong correlations in all 3 tests were interpreted as having experienced trophic growth with little to no geographic movement, eliminating 1 of 2 possible interpretations for the isotope profiles in Fig. 2. We acknowledge that this approach is subject to both Type I and Type II errors but represents one possible way of moving from a population-level to an individual-level interpretation.

3. RESULTS

3.1. Biological and isotopic comparisons between species

Red grouper ranged from 29.2 to 78.1 cm FL and 2–10 yr old, with 1 fish unaged. Tilefish ranged from 48 to 99 cm FL and 8–20 yr old, with 4 fish unaged (Tables S1 & S2). Multiple linear regression (R Core Team 2019) did not detect a relationship between FL and capture depth or capture latitude for either species (tilefish: $F_{2,33} = 2.38$, $R^2 = 0.13$, $p = 0.108$; red grouper: $F_{2,26} = 0.06$, $R^2 = 0.01$, $p = 0.95$).

Multivariate isotope location was significantly different between the 2 species ($F = 923.56$, $R^2 = 0.49$, $p < 0.001$; Fig. 3), as was multivariate dispersion ($F = 14.60$, $p < 0.001$). Tilefish mean (\pm SE) eye-lens $\delta^{15}\text{N}$

Table 1. Rules of interpretation for all possible correlation outcomes within the eye-lens isotopic profiles of individual fish and capture location as a function of length for the species. ELD: eye-lens diameter. Correlation = Spearman rank correlation applied to the entire lifetime eye-lens isotopic profiles for an individual fish, or species, as indicated

1. $\delta^{15}\text{N}$ value correlation with ELD (within individuals)
 - 1A. If $\delta^{15}\text{N}$ value negatively correlates with ELD, then individual reduced trophic position or moved against $\delta^{15}\text{N}$ gradient.
 - 1B. If $\delta^{15}\text{N}$ value positively correlates with ELD, then individual increased trophic position or moved with $\delta^{15}\text{N}$ gradient.
 - 1C. If $\delta^{15}\text{N}$ value does not significantly correlate with ELD, then trophic position or movement along $\delta^{15}\text{N}$ gradient was inconsistent or did not change.
2. $\delta^{13}\text{C}$ value correlation with ELD (within individuals)
 - 2A. If $\delta^{13}\text{C}$ value negatively correlates with ELD, then individual reduced trophic position or moved against $\delta^{13}\text{C}$ gradient.
 - 2B. If $\delta^{13}\text{C}$ value positively correlates with ELD, then individual increased trophic position or moved with $\delta^{13}\text{C}$ gradient.
 - 2C. If $\delta^{13}\text{C}$ value does not significantly correlate with ELD, then trophic position, basal resource, and movement were inconsistent or did not change.
3. Capture fork length (FL) correlation with relative capture location (within species)
 - 3A. If capture length correlates (positively or negatively) with capture location, then the species tended to have directional movement.
 - 3B. If capture length does not correlate with relative capture position, then the species tended to be stationary or moved inconsistently.
4. $\delta^{13}\text{C}$ value correlation with $\delta^{15}\text{N}$ value (within individuals)
 - 4A. If $\delta^{13}\text{C}$ value negatively correlates with $\delta^{15}\text{N}$ value, then the individual (or its prey) moved against one isotopic gradient and with the other.
 - 4B. If $\delta^{13}\text{C}$ value positively correlates with $\delta^{15}\text{N}$ value, then the individual remained largely stationary while increasing trophic position.
 - 4C. If $\delta^{13}\text{C}$ value does not correlate with $\delta^{15}\text{N}$ value, then the individual (or its prey) moved inconsistently or was both stationary and did not change trophic position.

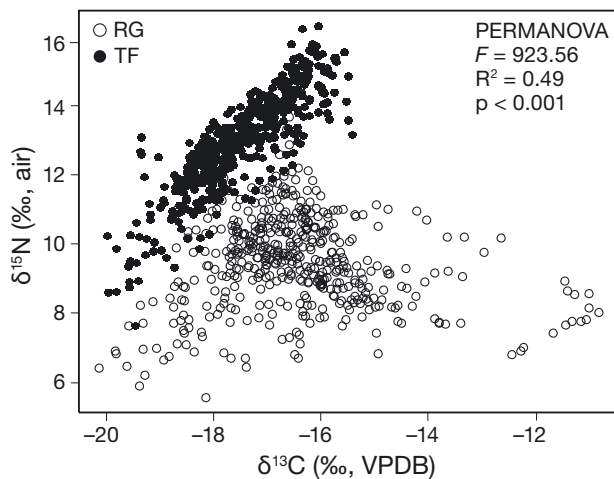


Fig. 3. Isotopic distribution for all red grouper (RG) and tilefish (TF) eye-lens laminae combined. PERMANOVA results comparing the difference in $\delta^{15}\text{N}$ and $\delta^{13}\text{C}$ by species are listed. Results are presented relative to international standards Vienna Pee Dee Belemnite (VPDB) for carbon and air for nitrogen

values and $\delta^{13}\text{C}$ values were 12.97 ± 0.07 and -17.49 ± 0.04 , respectively. Red grouper eye-lens $\delta^{15}\text{N}$ and $\delta^{13}\text{C}$ were 9.46 ± 0.06 and -16.49 ± 0.06 , respectively. In both red grouper and tilefish, ELD had positive,

logarithmic relationships with $\delta^{13}\text{C}$ and $\delta^{15}\text{N}$ values (Table 2, Fig. 4). Fits were over $R^2 = 0.5$ between ELD and tilefish $\delta^{13}\text{C}$, tilefish $\delta^{15}\text{N}$, and red grouper $\delta^{15}\text{N}$. However, red grouper $\delta^{13}\text{C}$ values were not well represented by this model ($R^2 = 0.12$; Table 2, Fig. 4). We found a positive linear relationship between tilefish $\delta^{15}\text{N}$ and $\delta^{13}\text{C}$ in the form $\delta^{15}\text{N} = a + b \times \delta^{13}\text{C}$ (Table 3, Fig. 5A). However, the linear mixed model for the relationship between $\delta^{15}\text{N}$ and $\delta^{13}\text{C}$ in red grouper failed to converge (Fig. 5B).

3.2. Relationships between ELD, $\delta^{13}\text{C}$, and $\delta^{15}\text{N}$ at the individual level

Individual red grouper eye-lens $\delta^{15}\text{N}$ increased as the fish grew (mean $\Delta\delta^{15}\text{N} \pm \text{SE} = 3.60 \pm 0.20\text{‰}$). Despite red grouper average increases in $\delta^{13}\text{C}$ over the lifetime ($1.93 \pm 0.22\text{‰}$), visual inspection indicated that most profiles peaked near 2 mm ELD (Fig. S1). The mean correlation between $\delta^{15}\text{N}$ and ELD was $r_s = 0.75$ ($p < 0.001$) and the mean correlation between $\delta^{13}\text{C}$ and ELD was $r_s = 0.29$ ($p = 0.50$). Correlations between $\delta^{15}\text{N}$ and ELD were positive and significant in all individuals, while $\delta^{13}\text{C}$ and ELD were positive and

Table 2. Statistics for nonlinear least-squares regression for isotopic values ($\delta^{15}\text{N}$ or $\delta^{13}\text{C}$) as a function of eye lens diameter (ELD) in both tilefish and red grouper. These regressions took the form of $\delta^{15}\text{N}$ or $\delta^{13}\text{C} = a + b \times \ln(\text{ELD})$ (see Section 2.2.1 for more details)

Regressed with ELD	n	a (\pm SE)	b (\pm SE)	F	p	R ²
Tilefish $\delta^{15}\text{N}$	468	11.02 \pm 0.07	1.54 \pm 0.05	1069	\leq 0.001	0.70
Tilefish $\delta^{13}\text{C}$	468	-18.59 \pm 0.05	0.86 \pm 0.04	496	\leq 0.001	0.52
Red grouper $\delta^{15}\text{N}$	406	8.12 \pm 0.07	1.28 \pm 0.06	526	\leq 0.001	0.57
Red grouper $\delta^{13}\text{C}$	406	-17.27 \pm 0.11	0.68 \pm 0.09	56	\leq 0.001	0.12

significant for 10 of 30 fish (Table S1). Profiles of eye-lens $\delta^{15}\text{N}$ as a function of $\delta^{13}\text{C}$ for each individual were highly variable in both slope and direction (Fig. S2). Five of 30 red grouper appeared to increase their trophic positions while remaining stationary and continuing to depend on similar basal resources, while the remainder appeared to move substantial distances across isotopic gradients and/or change their basal-resource dependence (Table S1).

In each individual tilefish eye lens, there was an increase in $\delta^{13}\text{C}$ and $\delta^{15}\text{N}$ values during life. Lifetime $\Delta\delta^{13}\text{C}$ was $2.50 \pm 0.12\text{‰}$ (mean \pm SE) and lifetime

$\Delta\delta^{15}\text{N}$ was $4.67 \pm 0.17\text{‰}$ (Fig. S2). Average tilefish correlation between $\delta^{15}\text{N}$ and ELD was $r_s = 0.80$ ($p < 0.001$), and correlation between $\delta^{13}\text{C}$ and ELD was $r_s = 0.70$ ($p < 0.001$). Average correlation between $\delta^{13}\text{C}$ and $\delta^{15}\text{N}$ was $r_s = 0.86$ ($p < 0.001$; Table S2) within individual fish. Nearly all (35 out of 36) tilefish appeared to increase their trophic positions during life while remaining in the same location and feeding within the same basal-resource regime. Only the smallest tilefish was suspected of a change in basal-resource dependence based on these rules (Table S2).

Table 3. Statistics for linear mixed model of $\delta^{15}\text{N}$ value as a function of $\delta^{13}\text{C}$ value in both tilefish and red grouper. All regressions took the form of $\delta^{15}\text{N} = a + b \times \delta^{13}\text{C}$

Species	n	a (\pm SE)	b (\pm SE)	Permuted p
Tilefish	468	39.45 \pm 1.05	1.51 \pm 0.06	0.001
Red grouper	406	Model did not converge		

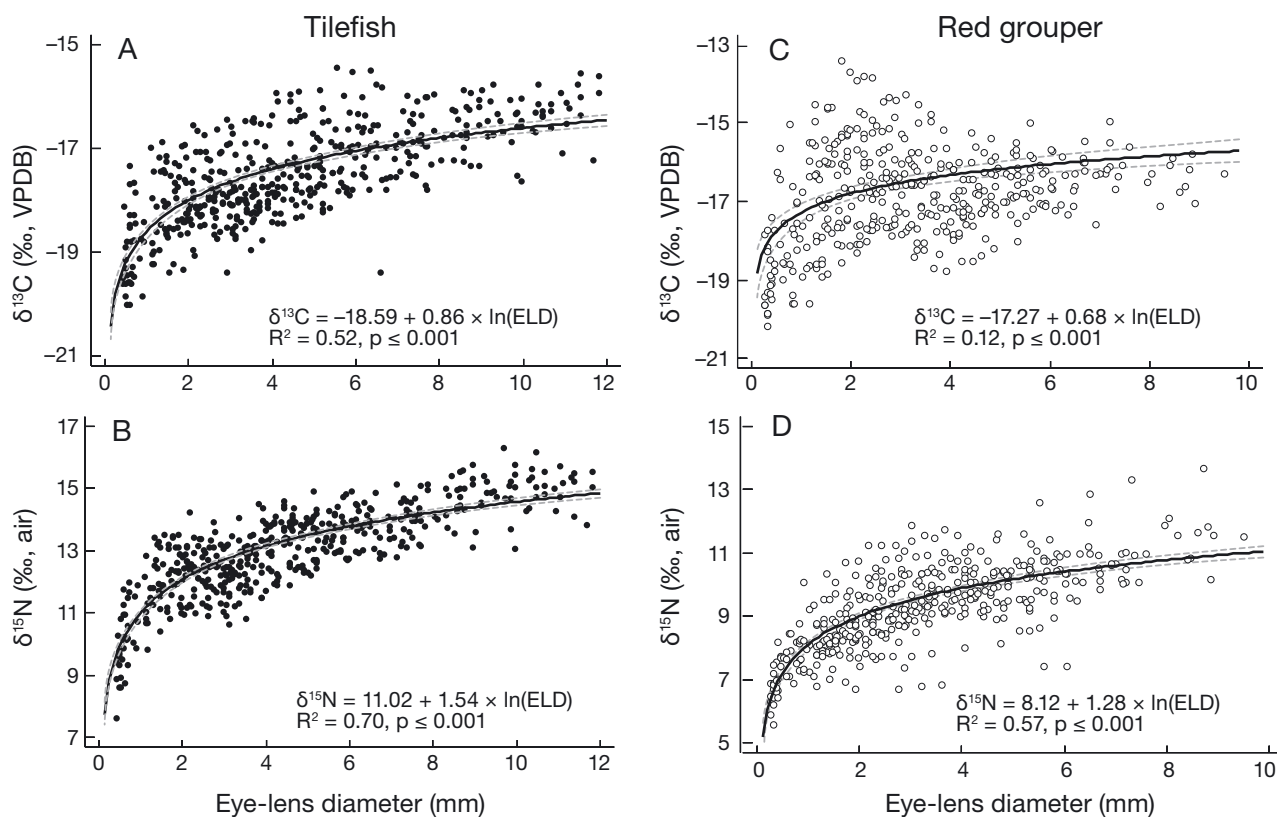


Fig. 4. Non-linear regression of $\delta^{15}\text{N}$ and $\delta^{13}\text{C}$ as a function of eye-lens diameter (ELD) for (A,B) tilefish and (C,D) red grouper. Results are presented relative to international standards Vienna Pee Dee Belemnite (VPDB) for carbon and air for nitrogen. Gray dashed lines represent 95% confidence interval for the non-linear regression model

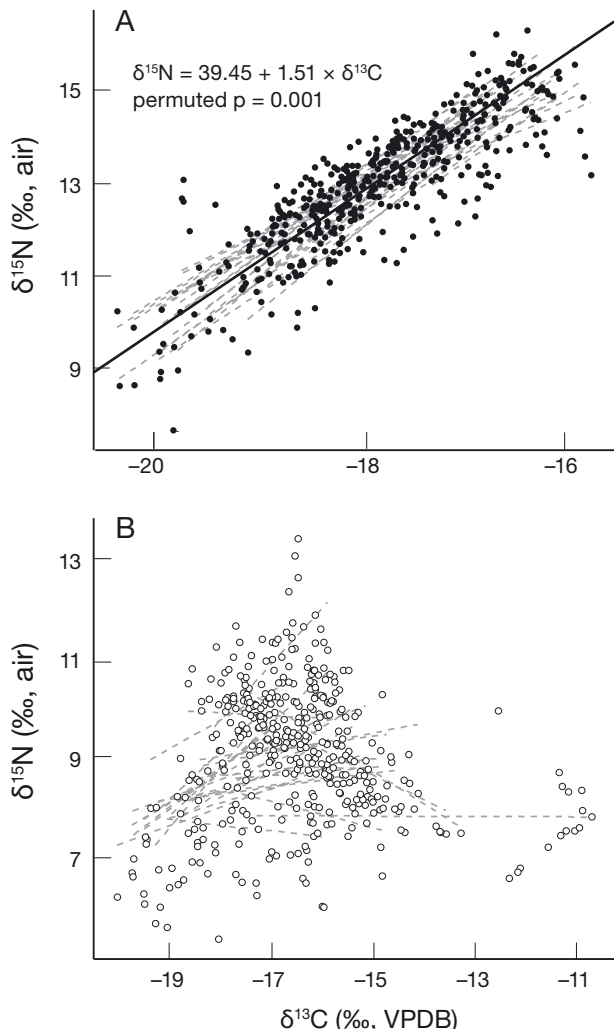


Fig. 5. Linear mixed-effects model relating eye-lens $\delta^{13}\text{C}$ values to eye-lens $\delta^{15}\text{N}$ values using individual fish as a random effect within the model. The regression is in the form $\delta^{15}\text{N} = a + b \times \delta^{13}\text{C}$ (see Section 2.2.1 for more details). Dashed gray lines indicate the slope of the model computed for each individual fish. (A) Tilefish. The equation at the top of the panel represents the average model built using all individuals, and the solid black line shows this model. The non-linear permuted p-value is shown. (B) Red grouper. No average model is given because the model failed to converge for this species

4. DISCUSSION

We used the isotope profiles reconstructed from fish eye lenses as a novel approach for detecting ontogenetic habitat shifts. We took advantage of the spatially decoupled isoscapes of fish tissue $\delta^{13}\text{C}$ and $\delta^{15}\text{N}$ values in the eastern Gulf of Mexico (Fig. 1A) to interpret eye-lens isotope profiles as movement on a lifetime scale. We used tilefish, a lifelong burrow-inhabiting species, as a model of a stationary species. We contrasted the isotope profiles in these eye lenses

with those of red grouper, which are known to move inshore and then offshore across the West Florida Shelf with changing ontogeny. The shapes of eye-lens isotope profiles and correlations between isotopes, coupled with the orthogonal isotopic background, suggest that similar patterns of movement could be detected for any species living in an area with similarly decoupled isotopic backgrounds.

Differences in overall isotopic values between tilefish and red grouper (Fig. 3) follow background trends in $\delta^{13}\text{C}$ and $\delta^{15}\text{N}$ values for the region (Fig. 1A). Tilefish in the Gulf of Mexico inhabit a narrow geographic range in areas that have a steep depth gradient (Steimle et al. 1999, Pierdomenico et al. 2015). All tilefish in this study were collected at depths of 178–375 m, with little cross-shelf distribution (Fig. 1B), which is reflected in their relatively high, tightly grouped $\delta^{13}\text{C}$ and $\delta^{15}\text{N}$ values. Red grouper occur on patchy reef habitats of the West Florida Shelf (Moe 1969, Coleman et al. 2010), usually in waters <100 m depth (SEDAR 2015). All red grouper in this study were collected in 10–40 m to the east and southeast of tilefish collections (Fig. 1B). The wide range of eye-lens $\delta^{13}\text{C}$ values in red grouper reflects cross-shelf movement over time, and the low eye-lens $\delta^{15}\text{N}$ values reflect their reliance on more southern habitats than tilefish (Figs. 1B & 3).

In order to enhance interpretation and broaden applications of eye-lens stable isotope data, we developed an approach that established generalized rules of interpretation (Table 1, Fig. 2). We first segregated the potential effects of trophic change and movement on fish eye-lens isotope values, and then recombined these effects to simulate all possible isotopic outcomes (Fig. 2), similar to Meath et al. (2019). We expanded this exercise to include all possible correlations between isotope values and fish length, using ELD as a proxy (Table 1).

We observed the lowest $\delta^{15}\text{N}$ values during the earliest phases of exogenous feeding in both species, which is consistent with previous eye-lens isotope findings (Wallace et al. 2014, Quaeck-Davies et al. 2018, Simpson et al. 2019). In both species, $\delta^{15}\text{N}$ fit a logarithmic function of ELD (Table 2, Fig. 4), with isotope values increasing at a faster rate during early life, similar to trends in fish body length (Juanes 2016) and in agreement with a recent fish eye-lens isotope study (Curtis et al. 2020). One mechanism for trophic increase with body growth is the addition of larger prey to the available prey pool as gape limitation decreases (Dalponti et al. 2018). In addition, large individuals at higher trophic positions, which are capable of substituting different trophic path-

ways into their diets, reduce vulnerability to basal-resource instability (MacKenzie et al. 2012, Burghart et al. 2013, Dalponti et al. 2018).

At the individual level, Spearman rank correlations were significant between $\delta^{15}\text{N}$ values and ELD in all 36 individual tilefish and in 27 of 30 red grouper (90%). There was no significant correlation between $\delta^{15}\text{N}$ value and ELD in 3 red grouper, suggesting that some individuals either did not increase their trophic positions or they moved far enough (southward) to isotopically negate the increase in $\delta^{15}\text{N}$ value expected from trophic growth. Red grouper tagging studies have shown that substantial movement is uncommon for adults over a 1–2 yr time period (Burns & Froeschke 2012), but some individuals have been shown to move >50 km southward, a distance sufficient to offset the $\delta^{15}\text{N}$ value increase from trophic growth on the West Florida Shelf (Burns 2009).

The logarithmic model relating tilefish eye-lens $\delta^{13}\text{C}$ value to ELD fit the data well, as did Spearman rank correlations between $\delta^{13}\text{C}$ value and ELD for individuals, suggesting consistent growth with little movement over time (Table 2, Fig. 4). The red grouper logarithmic model did not have a tight fit (Table 2, Fig. 4), and $\delta^{13}\text{C}$ values did not correlate significantly with ELD in most individuals. Many of the non-significant relationships were due to peaks in the $\delta^{13}\text{C}$ values during early life (Fig. S1), potentially revealing ontogenetic changes in habitat use and/or basal-resource dependence by moving inshore and then back offshore before sexual maturity (Keough et al. 1998, Araújo et al. 2007, Ellis et al. 2014).

Trophic fractionation without concurrent movement over time couples $\delta^{13}\text{C}$ to $\delta^{15}\text{N}$ values in a lifetime record such as eye lenses. Both $\delta^{13}\text{C}$ and $\delta^{15}\text{N}$ increase together as trophic position changes. Based on data from other marine mesopredators, the slope of this relationship would be approximately 1.0–1.7 (McCutchan et al. 2003, Matley et al. 2016, Eddy 2019). However, the linear relationship between tissue isotopes is disrupted if the fish move across isoscapes that are not spatially correlated with one another (i.e. the processes that control them are decoupled), as is the case in the $\delta^{13}\text{C}$ and $\delta^{15}\text{N}$ isoscapes on the West Florida Shelf. Thus, our proposed explanation for correlations in tilefish eye lenses (Fig. 5A; Fig. S4) is increased trophic position as mouth gape increases, coupled with a lack of movement along either isoscape. Indeed, the average slope of the relationship between $\delta^{15}\text{N}$ and $\delta^{13}\text{C}$ was 1.5‰ in this species (Fig. 5A), within the range of values expected for marine mesopredators. Whereas trophic growth can also be observed in red grouper eye-lens $\delta^{15}\text{N}$ profiles

(Fig. 4C; Fig. S1), correlations between $\delta^{13}\text{C}$ and $\delta^{15}\text{N}$ values are weak in this species (Fig. S2), and no linear relationship existed between the 2 isotopes (Fig. 5B; Fig. S2). Taken together, these data suggest that most individual red grouper moved considerable distances across the $\delta^{13}\text{C}$ isoscape during their lifetimes.

The eye-lens isotope profiles observed in tilefish and red grouper are consistent with available life history and diet information for the 2 species. In future studies of fish eye-lens isotopes, we suggest using models to investigate changes in trophic position, basal-resource dependence, and movement in populations as a whole, and a series of correlations to evaluate trends within individuals. In areas where $\delta^{13}\text{C}$ and $\delta^{15}\text{N}$ values are not spatially correlated, we suggest that a strong correlation between $\delta^{13}\text{C}$ and $\delta^{15}\text{N}$ values in eye-lens profiles serves as an indicator of high site fidelity during trophic growth, especially when a linear relationship between the 2 isotope profiles has a slope between 1.0 and 1.7. In contrast, a weak correlation between the profiles of these 2 isotopes and a lack of linear relationship indicates ontogenetic movement across spatially variable isoscapes. Individuals with weak correlations and slopes outside this range can then be investigated for ontogenetic habitat or diet shifts using methods such as diet analysis, compound-specific stable isotope analyses of eye-lens laminae (Wallace 2019), tagging studies, or other combinations of analysis types. Our approach provides a promising alternative to subjective interpretation of lifetime isotope profiles. Taking a weight-of-evidence approach (i.e. by analyzing multiple individuals and coupling isotope data with other types of data) strengthens the interpretation. This method could be applied to species for which other life history information is lacking, providing a simple means of detecting ontogenetic movement in poorly studied species.

Acknowledgements. We recognize the important intellectual contributions made to this effort by the late David J. Hollander (University of South Florida College of Marine Science [USFCMS]). This research was supported by the Florida RESTORE Act Centers of Excellence Program, administered by the Florida Institute of Oceanography (USF awards 4710112604 and 4710112901), and by the BP/Gulf of Mexico Research Initiative (GOMRI) via the C-IMAGE research consortium. As part of C-IMAGE, Dr. Steve Murawski (USFCMS) conducted the longline sampling with the assistance of the captain and crew of the RV 'Weatherbird II,' operated by the Florida Institute of Oceanography, along with its scientific crew, notably Amy Wallace, Susan Snyder, Kristina Deak, and Elizabeth Herdter (all USFCMS). Laboratory assistance was provided by Catherine Bruger (Ocean Conservancy). Tilefish ages were provided by Greta Helmueller, and red grouper ages were provided by Mike

Schram (both USFCMS). Ethan Goddard and Nico Zenzola (USFCMS) conducted the stable isotope analyses. All fish collections and tissue dissections were supported by research collecting permits and IACUC protocols at the University of South Florida. All data are published on the Gulf of Mexico Research Initiative Information and Data Cooperative (GRIIDC) website (<https://data.gulfresearchinitiative.org/data/R1.x135.120:0012>).

LITERATURE CITED

- Able KW, Grimes CB, Cooper RA, Uzmann JR (1982) Burrow construction and behavior of tilefish, *Lopholatilus chamaeleonticeps*, in Hudson submarine canyon. *Environ Biol Fishes* 7:199–205
- Able KW, Twichell DC, Grimes CB, Jones RS (1987) Tilefishes of the genus *Caulolatilus* construct burrows in the sea floor. *Bull Mar Sci* 40:1–10
- Ainsworth CH, Schirripa MJ, Luna HNM (2015) An ATLANTIS ecosystem model for the Gulf of Mexico supporting integrated ecosystem assessment. NOAA Tech Memo NMFS-SEFSC-676
- Araújo MS, Bolnick DI, Machado G, Giarretta AA, dos Reis SF (2007) Using $\delta^{13}\text{C}$ stable isotopes to quantify individual-level diet variation. *Oecologia* 152:643–654
- Bates D, Mächler M, Bolker BM, Walker SC (2015) Fitting linear fixed effect models using lme4. *J Stat Softw* 67: 1–48
- Brule T, Canche LGR (1993) Food habits of juvenile red groupers, *Epinephelus morio* (Valenciennes, 1828) from Campeche bank, Yucatan, Mexico. *Bull Mar Sci* 52: 772–779
- Buchheister A, Latour RJ (2010) Turnover and fractionation of carbon and nitrogen stable isotopes in tissues of a migratory coastal predator, summer flounder (*Paralichthys dentatus*). *Can J Fish Aquat Sci* 67:445–461
- Buchheister A, Latour RJ (2011) Trophic ecology of summer flounder in lower Chesapeake Bay inferred from stomach content and stable isotope analyses. *Trans Am Fish Soc* 140:1240–1254
- Bullock LH, Smith GB (1991) Seabasses (Pisces: Serranidae). *Mem Hourglass Cruises* 8:1–243
- Burghart SE, Jones DL, Peebles EB (2013) Variation in estuarine consumer communities along an assembled eutrophication gradient: implications for trophic instability. *Estuaries Coasts* 36:951–965
- Burns K (2009) Evaluation of the efficacy of the minimum size rule in the red grouper and red snapper fisheries with respect to J and circle hook mortality and barotrauma and the consequences for survival and movement. PhD dissertation, University of South Florida, Tampa, FL
- Burns KM, Froeschke JT (2012) Survival of red grouper (*Epinephelus morio*) and red snapper (*Lutjanus campechanus*) caught on J-hooks and circle hooks in the Florida recreational and recreational-for-hire fisheries. *Bull Mar Sci* 88: 633–646
- Coleman FC, Koenig CC, Scanlon KM, Heppell S, Heppell S, Miller MW (2010) Benthic habitat modification through excavation by red grouper, *Epinephelus morio*, in the northeastern Gulf of Mexico. *Open Fish Sci J* 3:1–15
- Coleman FC, Scanlon KM, Koenig CC (2011) Groupers on the edge: shelf edge spawning habitat in and around marine reserves of the northeastern Gulf of Mexico. *Prof Geogr* 63:456–474
- Curtis JS, Albins MA, Peebles EB, Stallings CD (2020) Stable isotope analysis of eye lenses from invasive lionfish yields record of resource use. *Mar Ecol Prog Ser* 637: 181–194
- Dahlgren CP, Eggleston DB (2001) Spatio-temporal variability in abundance, size and microhabitat associations of early juvenile Nassau grouper *Epinephelus striatus* in an off-reef nursery system. *Mar Ecol Prog Ser* 217:145–156
- Dalponti G, Guariento RD, Caliman A (2018) Hunting high or low: body size drives trophic position among and within marine predators. *Mar Ecol Prog Ser* 597:39–46
- Dance KM, Rooker JR, Shipley JB, Dance MA, Wells RJD (2018) Feeding ecology of fishes associated with artificial reefs in the northwest Gulf of Mexico. *PLOS ONE* 13: e0203873
- Eddy C (2019) Trophic discrimination factors for invasive lionfish (*Pterois volitans* and *P. miles*) in Bermuda. *Biol Invasions* 21:3473–3477
- Eldridge PJ (1988) The southeast area monitoring and assessment program (SEAMAP)—a state–federal–university program for collection, management, and dissemination of fishery-independent data and information in the southeastern United States. *Mar Fish Rev* 50:29–39
- Ellis R (2019) Red grouper (*Epinephelus morio*) shape faunal communities via multiple ecological pathways. *Diversity (Basel)* 11:89
- Ellis GS, Herbert G, Hollander DJ (2014) Reconstructing carbon sources in a dynamic estuarine ecosystem using oyster amino acid $\delta^{13}\text{C}$ values from shell and tissue. *J Shellfish Res* 33:217–225
- Ellis RD, Coleman FC, Koenig CC (2017) Effects of habitat manipulation by red grouper, *Epinephelus morio*, on faunal communities associated with excavations in Florida Bay. *Bull Mar Sci* 93:961–983
- Fahay MP (1983) Guide to the early stages of marine fishes occurring in the western north Atlantic Ocean, Cape Hatteras to the southern Scotian Shelf. *J Northwest Atl Fish Sci* 4:1–423
- Farmer NA, Ault JS (2014) Modeling coral reef fish home range movements in Dry Tortugas, Florida. *Sci World J* 2014:629791
- Fisher JAD, Frank KT, Petrie B, Leggett WC (2014) Life on the edge: environmental determinants of tilefish (*Lopholatilus chamaeleonticeps*) abundance since its virtual extinction in 1882. *ICES J Mar Sci* 71:2371–2378
- Fry B (2006) Stable isotope ecology. Springer Science+Business Media, New York, NY
- Fry B, Wainright SC (1991) Diatom sources of ^{13}C -rich carbon in marine food webs. *Mar Ecol Prog Ser* 76:149–157
- Golikov AV, Ceia FR, Sabirov RM, Zaripova ZI, Blicher ME, Zakharov DV, Xavier JC (2018) Ontogenetic changes in stable isotope ($\delta^{13}\text{C}$ and $\delta^{15}\text{N}$) values in squid *Gonatus fabricii* (Cephalopoda) reveal its important ecological role in the Arctic. *Mar Ecol Prog Ser* 606:65–78
- Graham BS, Grubbs D, Holland K, Popp BN (2007) A rapid ontogenetic shift in the diet of juvenile yellowfin tuna from Hawaii. *Mar Biol* 150:647–658
- Granneman JE (2018) Evaluation of trace-metal and isotopic records as techniques for tracking lifetime movement patterns in fishes. PhD dissertation, University of South Florida, Tampa, FL
- Grasty S, Wall CC, Gray JW, Brizzolaro J, Murawski SA (2019) Temporal persistence of red grouper holes and analysis of associated fish assemblages from towed camera data in the Steamboat Lumps Marine Protected Area.

- Trans Am Fish Soc 148:652–660
- Grimes CB (1983) A technique for tagging deepwater fish. Fish Bull 81:663–666
- Grimes CB, Able KW, Jones RS (1986) Tilefish, *Lopholatilus chamaeleonticeps*, habitat, behavior and community structure in md-Atlantic and southern New England waters. Environ Biol Fishes 15:273–292
- ✦ Grippio MA, Fleeger JW, Dubois SF, Condrey R (2011) Spatial variation in basal resources supporting benthic food webs revealed for the inner continental shelf. Limnol Oceanogr 56:841–856
- Grossman GD, Harris MJ, Hightower JE (1985) The relationship between tilefish, *Lopholatilus chamaeleonticeps*, abundance and sediment composition off Georgia. Fish Bull 83:443–447
- ✦ Grüss A, Schirripa MJ, Chagaris D, Velez L and others (2016) Estimating natural mortality rates and simulating fishing scenarios for Gulf of Mexico red grouper (*Epinephelus morio*) using the ecosystem model OSMOSE-WFS. J Mar Syst 154:264–279
- ✦ Grüss A, Thorson JT, Sagarese SR, Babcock EA, Karnauskas M, Walter JF III, Drexler M (2017) Ontogenetic spatial distributions of red grouper (*Epinephelus morio*) and gag grouper (*Mycteroperca microlepis*) in the US Gulf of Mexico. Fish Res 193:129–142
- ✦ Hansson S, Hobbie JE, Elmgren R, Larsson U, Fry B, Johansson S (1997) The stable nitrogen isotope ratio as a marker of food-web interactions and fish migration. Ecology 78: 2249–2257
- ✦ Heady WN, Moore JW (2013) Tissue turnover and stable isotope clocks to quantify resource shifts in anadromous rainbow trout. Oecologia 172:21–34
- Hine AC, Locker SD (2011) The Florida Gulf of Mexico continental shelf—great contrasts and significant transitions. In: Buster NA, Holmes CW (eds) Gulf of Mexico: origin, waters, and marine life. Vol 3: Geology. Texas A&M University, College Station, TX, p 101–127
- ✦ Holtum JAM, Winter K (2014) Limited photosynthetic plasticity in the leaf-succulent CAM plant *Agave angustifolia* grown at different temperatures. Funct Plant Biol 41: 843–849
- Huelster S (2015) Comparison of isotope-based biomass pathways with groundfish community structure in the eastern Gulf of Mexico. MSc thesis, University of South Florida, Tampa, FL
- ✦ Johnson AG, Collins LA (1994) Age-size structure of red grouper, (*Epinephelus morio*), from the eastern Gulf of Mexico. Northeast Gulf Sci 13:101–106
- ✦ Juanes F (2016) A length-based approach to predator–prey relationships in marine predators. Can J Fish Aquat Sci 73:677–684
- ✦ Keough JR, Hagley CA, Ruzycski E, Sierszen M (1998) $\delta^{13}\text{C}$ composition of primary producers and role of detritus in a freshwater coastal ecosystem. Limnol Oceanogr 43: 734–740
- ✦ Kurth BN, Peebles EB, Stallings CD (2019) Atlantic tarpon (*Megalops atlanticus*) exhibit upper estuarine habitat dependence followed by foraging system fidelity after ontogenetic habitat shifts. Estuar Coast Shelf Sci 225: 106248
- ✦ Liu BL, Xu W, Chen XJ, Huan MY, Liu N (2020) Ontogenetic shifts in trophic geography of jumbo squid, *Dosidicus gigas*, inferred from stable isotopes in eye lens. Fish Res 226:105507
- ✦ Locker SD, Armstrong RA, Battista TA, Rooney JJ, Sherman C, Zawada DG (2010) Geomorphology of mesophotic coral ecosystems: current perspectives on morphology, distribution, and mapping strategies. Coral Reefs 29:329–345
- Lombardi-Carlson L (2014) Age and growth description of red grouper (*Epinephelus morio*) from the northeastern Gulf of Mexico: 1978–2013 SEDAR 42. SEDAR, North Charleston, SC
- ✦ Lombardi-Carlson LA, Andrews AH (2015) Age estimation and lead–radium dating of golden tilefish, *Lopholatilus chamaeleonticeps*. Environ Biol Fishes 98:1787–1801
- Lowerre-Barbieri S, Crabtree L, Switzer TS, McMichael RH Jr (2014) Maturity, sexual transition, and spawning seasonality in the protogynous red grouper on the West Florida Shelf SEDAR 42. SEDAR42-DW-7. SEDAR, North Charleston, SC
- ✦ Luo D, Ganesh S, Koolaard J (2020) Package Predictmeans for R Version 1.0.4. <https://CRAN.R-project.org/package=predictmeans>
- ✦ Lynnerup N, Kjeldsen H, Heegaard S, Jacobsen C, Heinemeier J (2008) Radiocarbon dating of the human eye lens crystallines reveal [sic] proteins without carbon turnover throughout life. PLOS ONE 3:e1529
- ✦ MacKenzie KM, Palmer MR, Moore A, Ibbotson AT, Beaumont WRC, Poulter DJS, Trueman CN (2011) Locations of marine animals revealed by carbon isotopes. Sci Rep 1:21
- ✦ MacKenzie KM, Trueman CN, Palmer MR, Moore A, Ibbotson AT, Beaumont WRC, Davidson IC (2012) Stable isotopes reveal age-dependent trophic level and spatial segregation during adult marine feeding in populations of salmon. ICES J Mar Sci 69:1637–1645
- ✦ Matley JK, Fisk AT, Tobin AJ, Heupel MR, Simpfendorfer CA (2016) Diet–tissue discrimination factors and turnover of carbon and nitrogen stable isotopes in tissues of an adult predatory coral reef fish, *Plectropomus leopardus*. Rapid Commun Mass Spectrom 30:29–44
- ✦ McClelland JW, Holl CM, Montoya JP (2003) Relating low $\delta^{15}\text{N}$ values of zooplankton to N_2 -fixation in the tropical North Atlantic: insights provided by stable isotope ratios of amino acids. Deep Sea Res I 50:849–861
- ✦ McCutchan JH, Lewis WM, Kendall C, McGrath CC (2003) Variation in trophic shift for stable isotope ratios of carbon, nitrogen, and sulfur. Oikos 102:378–390
- ✦ McMahon KW, Fogel ML, Elsdon TS, Thorrold SR (2010) Carbon isotope fractionation of amino acids in fish muscle reflects biosynthesis and isotopic routing from dietary protein. J Anim Ecol 79:1132–1141
- ✦ Meath B, Peebles EB, Seibel BA, Judkins H (2019) Stable isotopes in the eye lenses of *Doryteuthis plei* (Blainville 1823): exploring natal origins and migratory patterns in the eastern Gulf of Mexico. Cont Shelf Res 174:76–84
- Moe MAJ (1969) Biology of the red grouper *Epinephelus morio* from the eastern Gulf of Mexico. Florida Department of Natural Resources Marine Research Laboratory Professional Papers Series. Fish and Wildlife Research Institute, St. Petersburg, FL
- ✦ Mohan JA, Smith SD, Connelly TL, Attwood ET, McClelland JW, Herzka SZ, Walther BD (2016) Tissue-specific isotope turnover and discrimination factors are affected by diet quality and lipid content in an omnivorous consumer. J Exp Mar Biol Ecol 479:35–45
- ✦ Moncreiff CA, Sullivan MJ (2001) Trophic importance of epiphytic algae in subtropical seagrass beds: evidence from multiple stable isotope analyses. Mar Ecol Prog Ser 215:93–106

- ✦ Murawski SA, Peebles EB, Gracia A, Tunnell JW, Armenteros M (2018) Comparative abundance, species composition, and demographics of continental shelf fish assemblages throughout the Gulf of Mexico. *Mar Coast Fish* 10: 325–346
- Nicol JAC (1989) *The eyes of fishes*. Clarendon, Oxford
- ✦ Nielsen J, Hedeholm RB, Heinemeier J, Bushnell PG and others (2016) Eye lens radiocarbon reveals centuries of longevity in the Greenland shark (*Somniosus microcephalus*). *Science* 353:702–704
- ✦ O'Connor BS, Muller-Karger FE, Nero RW, Hu CM, Peebles EB (2016) The role of Mississippi River discharge in offshore phytoplankton blooming in the northeastern Gulf of Mexico during August 2010. *Remote Sens Environ* 173: 133–144
- ✦ Ogston G, Beatty SJ, Morgan DL, Pusey BJ, Lymbery AJ (2016) Living on burrowed time: aestivating fishes in south-western Australia face extinction due to climate change. *Biol Conserv* 195:235–244
- ✦ Oksanen J, Blanchet FG, Friendly M, Kindt R and others (2019) Vegan: community ecology package. R package version 2.5-4. <https://CRAN.R-project.org/package=vegan>
- Peebles EB, Hollander DJ (2020) Combining isoscapes with tissue-specific isotope records to recreate the geographic histories of fish. In: Murawski SA, Ainsworth CH, Gilbert S, Hollander DJ, Paris CB, Schlüter M, Wetzel DL (eds) *Scenarios and responses to future deep oil spills*. Springer, Cham, p 203–218
- ✦ Pierdomenico M, Guida VG, Macelloni L, Chiocci FL and others (2015) Sedimentary facies, geomorphic features and habitat distribution at the Hudson Canyon head from AUV multibeam data. *Deep Sea Res II* 121:112–125
- ✦ Post DM (2002) Using stable isotopes to estimate trophic position: models, methods, and assumptions. *Ecology* 83: 703–718
- ✦ Quaek-Davies K, Bendall VA, MacKenzie KM, Hetherington S, Newton J, Trueman CN (2018) Teleost and elasmobranch eye lenses as a target for life-history stable isotope analyses. *PeerJ* 6:e4883
- R Core Team (2019) R: A language and environment for statistical computing. Version 3.6.1. R Foundation for Statistical Computing, Vienna
- ✦ Radabaugh KR, Peebles EB (2014) Multiple regression models of $\delta^{13}\text{C}$ and $\delta^{15}\text{N}$ for fish populations in the eastern Gulf of Mexico. *Cont Shelf Res* 84:158–168
- ✦ Radabaugh KR, Hollander DJ, Peebles EB (2013) Seasonal $\delta^{13}\text{C}$ and $\delta^{15}\text{N}$ isoscapes of fish populations along a continental shelf trophic gradient. *Cont Shelf Res* 68:112–122
- Ricker WE (1975) Computation and interpretation of biological statistics of fish populations. *Bull Fish Res Board Can* 191
- Rinyu L, Janovics R, Molnar M, Kisvarday Z, Kemeny-Beke A (2020) Radiocarbon map of a bomb-peak labeled human eye. *Radiocarbon* 62:189–196
- ✦ Saul S, Die D, Brooks EN, Burns K (2012) An individual-based model of ontogenetic migration in reef fish using a biased random walk. *Trans Am Fish Soc* 141:1439–1452
- Scanlon KM, Coleman FC, Koenig CC (2005) Pockmarks on the outer shelf in the northern Gulf of Mexico: gas-release features or habitat modifications by fish? *Am Fish Soc Symp* 41:301–312
- SEDAR (SouthEast Data, Assessment, and Review) (2011) SEDAR 22—Gulf of Mexico Tilefish. SEDAR, North Charleston, SC
- SEDAR (2015) SEDAR 42 Stock Assessment Report—Gulf of Mexico Red Grouper. Report No. 42. SEDAR, North Charleston, SC
- ✦ Simpson SJ, Sims DW, Trueman CN (2019) Ontogenetic trends in resource partitioning and trophic geography of sympatric skates (Rajidae) inferred from stable isotope composition across eye lenses. *Mar Ecol Prog Ser* 624: 103–116
- Steimle FW, Zetlin CA, Berrien PL, Johnson DL, Sukwoo C (1999) Essential fish habitat source document: tilefish, *Lopholatilus chamaeleonticeps*, life history and habitat characteristics. National Marine Fisheries Service, Woods Hole, MA
- ✦ Stewart DN, Lango J, Nambiar KP, Falso MJS and others (2013) Carbon turnover in the water-soluble protein of the adult human lens. *Mol Vis* 19:463–475
- ✦ Sweeting CJ, Jennings S, Polunin NVC (2005) Variance in isotopic signatures as a descriptor of tissue turnover and degree of omnivory. *Funct Ecol* 19:777–784
- ✦ Tallamy DW, Pesek JD (1996) Carbon isotopic signatures of elytra reflect larval diet in luperine rootworms (Coleoptera: Chrysomelidae). *Environ Entomol* 25:1167–1172
- ✦ Trueman CN, Jackson AL, Chadwick KS, Coombs EJ and others (2019) Combining simulation modeling and stable isotope analyses to reconstruct the last known movements of one of Nature's giants. *PeerJ* 7:e7912
- von Bertalanffy L (1938) A quantitative theory of organic growth (Inquiries on growth laws. II). *Hum Biol* 10: 181–213
- ✦ Wall CC, Donahue BT, Naar DF, Mann DA (2011) Spatial and temporal variability of red grouper holes within Steamboat Lumps Marine Reserve, Gulf of Mexico. *Mar Ecol Prog Ser* 431:243–254
- Wallace AA (2019) *Recreating geographic and trophic histories of fish using bulk and compound-specific isotopes from eye lenses*. PhD dissertation, University of South Florida, Tampa, FL
- ✦ Wallace AA, Hollander DJ, Peebles EB (2014) Stable isotopes in fish eye lenses as potential recorders of trophic and geographic history. *PLOS ONE* 9:e108935
- Weaver DC (1996) *Feeding ecology and ecomorphology of three seabasses (Pisces: Serranidae) in the northeastern Gulf of Mexico*. MSc thesis, University of Florida, Gainesville, FL

Editorial responsibility: Stephen Wing,
Dunedin, New Zealand
Reviewed by: 3 anonymous referees

Submitted: April 15, 2020
Accepted: October 5, 2020
Proofs received from author(s): December 11, 2020